Adaptive Monogenic Filtering and Normalization of ESPI Fringe Patterns

J.A. Guerrero, J.L. Marroquin, M. Rivera

Centro de Investigación en Matemáticas
Apdo. Postal 402 Guanajuato, Gto. 36000, Mexico.
E-mail: jlm@fractal.cimat.mx

J.A. Quiroga

Depto. de Optica. Universidad Complutense de Madrid, 2841 Madrid, Spain

Abstract : This letter presents a technique for filtering and normalizing noisy fringe patterns which may include closed fringes, so that single-frame demodulation schemes may be successfully applied. It is based on the construction of an adaptive filter as a linear combination of the responses of a set of isotropic band-pass filters. The space-varying coefficients are proportional to the envelope of the response of each filter, which in turn is computed using the corresponding monogenic image (Felsberg and Sommer, IEEE TIP, 49(12):3136-3144, 2001). Some examples of demodulation of real ESPI patterns are presented.

OCIS Codes: 100.2000, 120.2650, 120.6160

The demodulation of single–frame fringe patterns containing closed fringes is an interesting problem, which has applications, for example, when the fringes are used to study fast transient phenomena. The difficulty of this problem stems from the fact that, although the absolute value of the local phase may be estimated from local (linear) operators – e.g., from the normalized intensity gradient – the determination of the phase sign requires tracking the local direction across the image, therefore is a global property [1, 2, 3, 4]. For this reason, demodulation algorithms are very sensitive to noise and local contrast variations, since even a small "bad" region may send the algorithm off track and have disastrous global consequences. This is true even when robust schemes, like the ones in [1, 4] are used for the demodulation of real noisy patterns, such as the ones obtained from ESPI. The purpose of this paper is to present an algorithm for producing, from real ESPI patterns with strong contrast variations, "clean", normalized patterns, which may be demodulated with existing procedures.

Given a locally monochromatic pattern, i.e., a pattern that locally looks like $A\cos(\omega_0 \cdot x + \phi)$, where A, ω_0 and ϕ are constants, corrupted with a white (wide-band) noise process, a narrow band band-pass filter tuned at ω_0 will effectively eliminate noise; moreover, if a quadrature filter pair is used (such as a complex-valued Gabor filter), one may obtain the local contrast A as the magnitude of the complex filter output, and hence, normalize the pattern by dividing it by A. It is possible that the local frequency has a substantial variation across the image, then a single filter will produce unreliable results in most places.

In theory, one may construct an adaptive filtering scheme by selecting a set of Gabor filters whose responses cover one half of the frequency plane, and constructing the output as a weighted combination of the real part of the responses of each filter, where the weights depend on the amplitude of the corresponding response; the problem is the passband of the filters must be narrow enough to have good noise reduction, but this scheme would require too many filters to have of practical use.

As an alternative, one may use isotropic bandpass filters that have annular frequency responses (see Fig. 1-a), so that the frequency plane may be covered using only a small set (we select, 5) of them. In this case, to obtain the local amplitude, one must use 2 companion filters whose frequency responses have odd symmetry (Figs. 1-b and 1-c). In particular, one may express the 2-D frequency vector $\omega = (\omega_1, \omega_2)^T$ in polar coordinates (ρ, θ), so that $\omega = (\rho \cos \theta, \rho \sin \theta)^T$; in this case, the 3 filters of Fig. 1 may be expressed in polar–separable form as:

$$
\begin{aligned}
H_{0k}(\rho, \theta) &= G(\rho - \rho_k) \\
H_{1k}(\rho, \theta) &= -iG(\rho - \rho_k) \sin(\theta) \\
H_{2k}(\rho, \theta) &= -iG(\rho - \rho_k) \cos(\theta)
\end{aligned}
\tag{1}
$$

where $G(\rho)$ is a bell–shaped function and ρ_k is the tuning frequency. The vector valued function $H_k = (H_{0k}, H_{1k}, H_{2k})^T$ is the frequency response of the k^{th} monogenic filter, and the vector-valued image $F_k = (F_{0k}, F_{1k}, F_{2k})^T$ that is obtained as the output of this filter is called the monogenic image [5]. One may easily verify that if a fringe pattern is locally monochromatic at pixel x, with local frequency $\omega_0 = (r_0 \cos t_0, r_0 \sin t_0)^T$, the k^{th} isotropic filter output will be $F_{0k}(x) = G(r_0 - \rho_k) A \cos(\omega_0 \cdot x + \phi)$, and the k^{th} monogenic image at this pixel will be a vector with magnitude $M_k(x) = G(r_0 - \rho_k)A$, this is independent of the orientation angle t_0. Taking K monogenic filters whose overlapping frequency responses covering the region of interest in the frequency plane (see Fig. 2), an adaptive filter can be constructed, whose output is a linear combination of the responses of the isotropic filters $\{H_{0k}, k = 1, \ldots, K\}$, with coefficients (weights) that depend on the corresponding magnitudes. The same weights may be used to find an "equivalent magnitude" that normalizes this output, obtaining the normalized pattern F as:

$$
F(x) = \frac{\sum_{k=1}^{K} w_k(x) F_{0k}(x)}{\sum_{k=1}^{K} w_k(x) M_k(x)} \tag{2}
$$

The weights w_k are computed as:

$$
w_k(x) = \left(\frac{M_k(x)}{M_{\max}(x)} \right)^p \tag{3}
$$

where $M_{\max}(x) = \max_k M_k(x)$ and p is a positive constant chosen so that $w_k(x)$ is close to 1 if $M_k(x) \approx M_{\max}(x)$, and is close to 0 otherwise. We have found that the results are practically insensitive from a precise value of p, as long as it is large enough (e.g., $p > 5$). All the results reported in here were obtained from experiments with $p = 10$.

It is important to note that in ESPI patterns, since speckle noise is multiplicative, bright fringes are more affected by it than dark ones. The filters we are proposing are linear — which implies that they manage bright and dark fringes in the same way — it is necessary to pre-process the image before they are applied, in a way that noise over bright fringes could be reduced. One simple way to do this is by means of a max-filter, whose output at pixel x is defined as:

$$I_M(x) = \max_{y \in W(x)} I(y)$$

where I is the input image, and $W(x)$ is a 3×3 window centered at pixel x. This filter has the effect of approximating the (upper) envelope of the pattern, and hence, reducing noise over the clear fringes. Also it has the unwanted effect of reducing the local contrast, however this is effectively counteracted by the adaptive filtering and normalization implemented by (2).

The detailed implementation of the monogenic filters is : As a first step, the frequency dynamic range $[\alpha, \beta]$ of the input image (in rad/pixel) is found by setting $\alpha = \pi/maxw$ and $\beta = \pi/minw$, where $maxw$, $minw$ are the widths (in pixels) of the widest and narrowest fringes of the pattern, respectively. We have developed a graphical interface where these values may be easily specified by the user, pointing at the limits of the desired fringes. Of these 2 values, the most critical is $maxw$: if it is too large, some narrow fringes may be lost in the reconstruction, and if it is too small, noise elimination over wide fringes may be incomplete. Note that if this filtering method is used in conjunction with a robust demodulation algorithm, such as [4], this residual noise will be futile for the final result, since it will be eliminated in the demodulation phase. In practice, one finds that underestimating $maxw$ up to an 80% of its true value, still produces good results, which means that an slightly underestimation in the interactive procedure could be safer. Note that these are the only parameters that the user has to specify. As a next step, for the bell-shaped function G we use:

$$\begin{aligned} G(\rho) &= \frac{1}{2}\left[1 + \sin\left(\frac{(h+2\rho)\pi}{2h}\right)\right] \text{ , for } \rho \in [-h, h] \\ &= 0 \text{ , otherwise} \end{aligned} \quad (4)$$

where $h = (\beta - \alpha)/(K - 1)$ (we take $K = 5$ filters in all cases). The filters are then computed using (1), with $\rho_k = \alpha + h(k-1)$, $k = 1, \ldots, K$. (when α is very small (4) has to be slightly modified, to guarantee that the responses of all filters are 0 for $\rho = 0$). Filtering is performed in the frequency domain, and the output magnitudes $\{M_k\}$ are smoothed with a Gaussian kernel (with $\sigma = 6$) before computing the weights using (3).

In figure 3 we present the results of the monogenic adaptive filtering and normalization of a sequence of ESPI patterns that correspond to the thermal deformation of a computer monitor. The processing time for the complete filtering and normalization procedure, for a 1024 X 1024 pixel image, was done in 50 sec. on a 3GHz workstation. To illustrate how this filtering effectively helps in the demodulation process, we also include the output (wrapped phase) of a state-of-the-art robust demodulation procedure, namely, the one in [4], applied to these filtered and normalized patterns. This method, which is, to our knowledge, the most robust demodulation procedure available for closed-fringe interferograms, starts by estimating the phase on a subregion of the image with relatively high quality open fringes, and iteratively extends this region using a variational approach, along directions where the fringes are better defined (highest quality regions). In this way, the phase in difficult regions, such as saddle points, or places where the fringes are too noisy or have gaps, are left undefined until there is enough information around them to interpolate reasonable values. This demodulation method is capable of recovering the correct phase, even when the fringes produced by the proposed preprocessing step are noisy or incomplete in small regions; if a simpler filtering and normalization preprocessing is applied, however, the method will fail. Thus, in Fig. 4 we depict the output of the same demodulation procedure applied to the first and last input images (first row of Fig. 3), after smoothing them with a Gaussian kernel and re-scaling their intensity to the interval $[-1, 1]$ (the results for the other images of the sequence are similar). Note that the standard filtering and normalization applied in this case cannot prevent the demodulation algorithm from getting an incorrect reconstruction (the recovered wrapped phase does not show 2π jumps at each fringe, as expected), which means that the proposed filtering and normalization procedure effectively increases the range of applicability of demodulation schemes for closed-fringe ESPI patterns, and may be very useful as a pre-processing step for other fringe pattern processing algorithms.

Acknowledgements: J.L. Marroquin and M. Rivera were supported in part by grants 46270 and 40722 from the Consejo Nacional de Ciencia y Tecnología, Mexico; J.A. Quiroga was supported by grant DPI2002-02104 from the Ministerio Español de Ciencia y Tecnología.

References

[1] M. Servin, J.L. Marroquin and J.A. Quiroga, "Regularized quadrature and phase tracking from a single closed-fringe interferogram" (JOSA A 21,3:411-419, 2004).

[2] K.G. Larkin, D.J. Bone and M.A. Oldfield, "Natural demodulation of two-dimensional fringe patterns. I. General background of the spiral phase quadrature transform" (JOSA A 18, 1862-1870, 2000).

[3] J. Kozlowsky and G. Serra, "Complex phase tracing method for fringe pattern demodulation" (Appl. Opt. 38:2256-2262, 1999).

[4] M. Rivera, Robust phase demodulation of interferograms with open or closed fringes (JOSA A 22,6: 1170-1175, 2005).

[5] M. Felsberg and G. Sommer, "The monogenic signal" (IEEE Transactions on Signal Processing, 49(12):3136-3144, 2001).

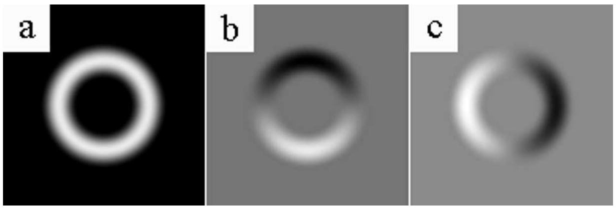

Figure 1: (a) Frequency response of an isotropic bandpass filter. (b) and (c) Imaginary part of the frequency response of the companion odd components of the monogenic filter.

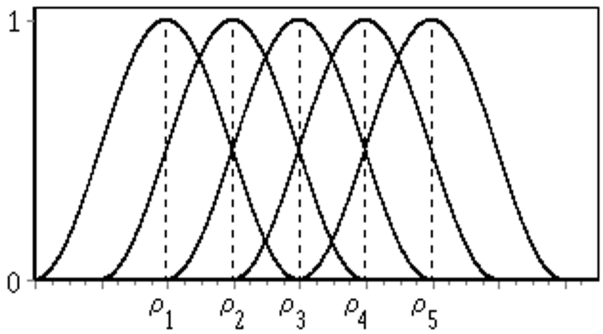

Figure 2: Magnitude of the response of the set of monogenic filters as a function of frequency magnitude.

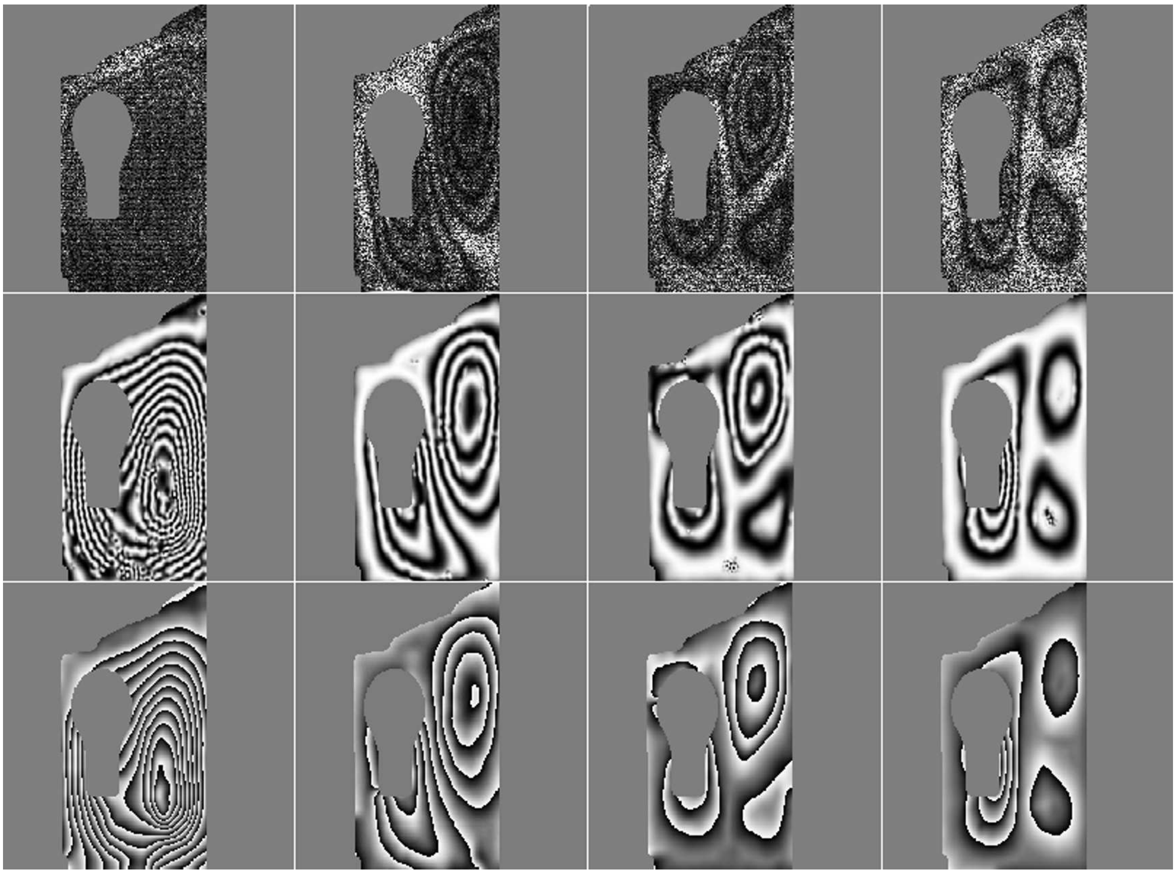

Figure 3: First row: sequence of ESPI patterns. Second row: filtered and normalized images. Third row: Output of a robust demodulation procedure (wrapped phase) applied to the second row.

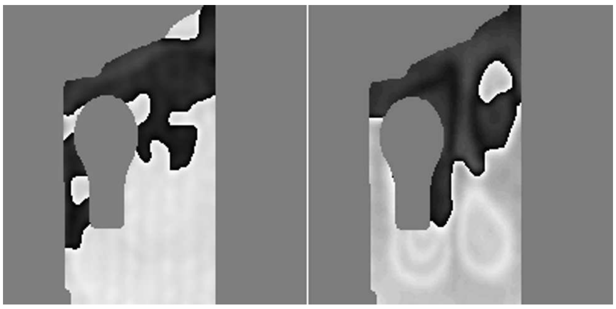

Figure 4: Output (wrapped phase) of the same robust demodulation procedure applied to the first and last images of the first row of fig. 3.